Short communication

In situ scanning tunneling microscopy study of the intergranular corrosion of copper

E. Martinez-Lombardia [a], L. Lapeire [b], V. Maurice [c],*, I. De Graeve [a], K. Verbeken [b], L.H. Klein [c], L.A.I. Kestens [b], P. Marcus [c],*, H. Terryn [a],**

[a] Research Group Electrochemical and Surface Engineering, Vrije Universiteit Brussel, Pleinlaan 2, 1050 Brussels, Belgium
[b] Department of Materials Science and Engineering, Ghent University (UGent), Technologiepark 903, Zwijnaarde, 9052 Ghent, Belgium
[c] Laboratoire de Physico-Chimie des Surfaces, CNRS (UMR 7045)-Chimie ParisTech, Ecole Nationale Supérieure de Chimie de Paris, 11 rue Pierre et Marie Curie, 75005 Paris, France

ARTICLE INFO

ABSTRACT

Electrochemical scanning tunneling microscopy is proved to be a powerful tool for providing valuable topographic information to study in situ the local corrosion properties of polycrystalline materials. It was applied to analyze the susceptibility to intergranular corrosion of different types of grain boundaries of microcrystalline copper in HCl and combined with electron backscatter diffraction to link the observed corrosion differences to a specific type of grain boundary. The superior resistance to intergranular corrosion of coherent twin boundaries over random grain boundaries is demonstrated.

1. Introduction

It is well known that grain boundary type has a big influence on the intergranular corrosion behavior of a polycrystalline material [1]. A "special boundary" is one that has better corrosion properties compared to a random boundary. These special boundaries are known as coincident site lattice boundaries (CSLs). CSL boundaries are denominated by the symbol Σn (1/n is the fraction of lattice points belonging to the coincident lattice). Some authors claim that apart from $\Sigma 3$ boundaries, the properties of CSLs in polycrystals are not different from random grain boundaries [2]. Moreover, it was demonstrated that $\Sigma 3$ boundaries do not necessary have good corrosion resistance properties. In 304 stainless steel, only coherent twin boundaries, $\Sigma 3$ boundaries with a {111} plane, were found to be resistant to intergranular corrosion [3]. It was also observed in austenitic steels subject to intergranular stress corrosion cracking that only the coherent twins were resistant to attack [4]. In our recently published work, the gold nanoplating technique confirmed the low grain boundary energy of the coherent twin boundaries on copper [5].

Various local electrochemical techniques have been applied for the investigation of the electrochemical behavior at grain boundaries of metals [6,7]. However, there are some limitations to their capabilities

mainly due to lateral resolution (around 20 μm). Ex situ scanning tunneling microscopy (STM) has already been used to study the atomic structure of a single grain boundary in graphite [8]. To date however, electrochemical STM (ECSTM) has never been used to observe in situ the intergranular corrosion evolution on a polycrystalline material although its application to corrosion studies of single-crystal materials is established [9–11].

In face centered cubic materials with low stacking fault energies, such as copper, it is possible to increase the amount of 'special' CSL boundaries by using special thermomechanical treatments [12,13]. Extensive studies have been conducted on deformation behavior of FCC materials at low temperature [14,15]. Here, cryogenic rolling, followed by annealing to ensure full recrystallization was used for manufacturing microcrystalline copper with a high grain boundary density and a high content of special $\Sigma 3^n$ grain boundaries [16,17]. The microstructure was quantified by EBSD and in situ ECSTM was applied to analyze the corrosion behavior of the different types of grain boundaries.

2. Experimental

Electrolytic Tough Pitch (ETP-) Cu, a high purity cast copper, with no traces of sulfur and minimal amounts of oxygen, was cryogenically rolled in liquid nitrogen with final thickness reduction of 91%. Annealing for 1 min at 200 °C ensured full recrystallization and suitable grain size and grain boundary density for the STM field of view. The surface was prepared by mechanical polishing with diamond paste down to 0.25 μm grade and electrochemical polishing in 60% orthophosphoric acid during 4 min at 1.4 V versus a copper electrode.

* Corresponding authors.
** Correspondence to: H. Terryn, Research Group Electrochemical and Surface Engineering, Vrije Universiteit Brussel, Pleinlaan 2, 1050 Brussels, Belgium.
E-mail addresses: Vincent-MAURICE@chimie-paristech.fr (V. Maurice), Philippe-MARCUS@chimie-paristech.fr (P. Marcus), Herman.Terryn@vub.ac.be (H. Terryn).

The microstructure of the samples was characterized by EBSD. The EBSD system is attached to an FEI® FE-SEM (Quanta) operated at 20 kV. Measurements were carried out with a step size of 0.1 μm and the orientation data were post-processed with the orientation imaging software package OIM-TSL®.

All ECSTM experiments were performed at room temperature with an Agilent Technologies PicoSPM system. The selected electrolyte was a non-deaerated 10 mM HCl aqueous solution. The sample was mounted in the ECSTM cell with a working electrode area of 0.16 cm², a Pt pseudoreference electrode and a Pt wire counter electrode. The tungsten STM tips were prepared from 0.25 mm diameter wire electrochemically etched in 3 M NaOH and covered by Apiezon wax. All images were obtained in the constant current mode. All potentials reported hereafter are relative to the standard hydrogen electrode (V/SHE).

The samples were exposed to the electrolyte at −0.05 V/SHE to avoid any copper dissolution before starting the experiments (open circuit potential of 0.1 V/SHE). They were then pre-treated with a scan down to −0.45 V/SHE (corresponding to the onset of hydrogen evolution) and upwards back to −0.05 V/SHE in order to fully reduce the air-formed oxide film. The topography of the metallic surface was then measured in a selected area. Afterwards, anodic dissolution was forced by scanning the potential in the positive direction till an anodic current density not exceeding 50 μA cm⁻² was measured. The potential was then scanned back to the starting value of −0.05 V/SHE and new images of the same area were taken at this potential. The evolution of the topography was thus followed after several anodic cycles.

A statistical study of the morphology and type of grain boundaries was used to link the in situ ECSTM data on intergranular corrosion behavior with a certain type of grain boundary.

3. Results and discussion

Fig. 1a shows the inverse pole figure (IPF) map of the microcrystalline copper sample. The average grain size is 1.1 μm. The image quality (IQ) map in Fig. 1b shows the different types of boundaries. Blue lines indicate random high angle boundaries (misorientation >15°) and red lines indicate all Σ3 boundaries. The length fraction of Σ3 boundaries is 51.2%. More detailed analysis reveals several long and parallel-sided Σ3 boundaries (pointed by black arrows). Most likely these are coherent twins since they are characterized by their parallel-sided arrangement [13]. In order to confirm this assumption, an area of 50×50 μm² was studied. Among 227 grain boundaries, only one straight grain boundary was found to be a random high angle boundary. All other straight

boundaries were found to be Σ3. On the other hand, when looking at the Σ3 boundaries, it was found that around 50% of them are straight and 50% are curved. It can be then concluded that a straight grain boundary has a very high probability to be a 'coherent twin boundary' and that a curved grain boundary can be cataloged either as random high angle boundary or non coherent Σ3 boundary.

Fig. 2a shows the cyclic voltammogram for the cathodic pre-treatment in the non-deaerated ECSTM cell. The reduction peak is observed at −0.20 V/SHE. The thickness (δ) of the cathodically reduced oxide layer was calculated from the charge density (q) of the reduction peak according to the Eq. (1):

$$\delta = qV/zF \qquad (1)$$

where V is the molar volume of the reduced oxide, F the Faraday constant and z the number of exchanged electrons. The measured reduction charge density is around 1000 μC cm⁻². Assuming that the oxide layer consists of Cu_2O (V = 23.9 cm³ mol⁻¹), the calculated thickness of the Cu_2O oxide layer is 2.7 nm. This is in agreement with the reported thickness of the air-formed oxide on copper of around 2.5 nm [18].

After cathodic reduction, anodic potentiodynamic polarization was performed, Fig. 2b, in order to induce dissolution of the copper metal and to produce intergranular corrosion. The STM tip was withdrawn from the surface while polarizing the sample and re-engaged afterwards allowing analyzing the very same area before and after several anodic cycles. From the anodic charge density transfer (129 μC cm⁻²), an equivalent thickness of ~0.1 nm of dissolved Cu(I) can be calculated using Eq. (1), which amounts to less than one equivalent monolayer. The cathodic peak measured at 0.08 V/SHE after dissolution most likely corresponds to deposition of dissolved copper. This process does not annihilate the local dissolution-induced modifications as shown below.

Fig. 3 shows the sample topography prior to (Fig. 3a) and after (Fig. 3b) 4 anodic scans. Two straight grain boundaries (marked by green arrows) can be seen together with several curved grain boundaries. The evolution of the different grain boundaries can be followed by cross section analysis. A considerable attack is observed for the curved grain boundary (height profile 2, Fig. 3d). The magnitude of intergranular corrosion is determined by both the penetration at the grain boundary and the dissolution at the surface of the grains that form the grain boundary. In this case, a significant depth penetration of 2 nm, equivalent to ~10 monolayers and much higher than measured electrochemically, is measured showing that dissolution proceeds essentially at grain boundaries in these conditions. Fig. 3c shows a height profile across the two straight grain boundaries. There is no indication of
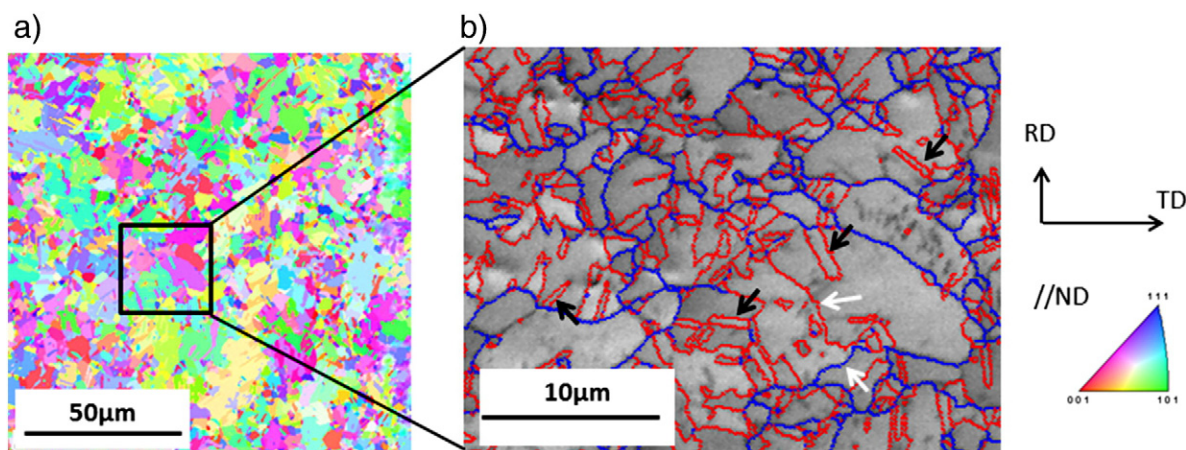

Fig. 1. (a) Inverse pole figure (IPF) map and (b) image quality (IQ) map of microcrystalline copper. In (b), blue lines denote random high angle boundaries (>15°) and red lines Σ3 boundaries. Coherent twins are marked with black arrows and random and non coherent Σ3 boundaries are marked with white arrows.